

## Role of Fragility in the Formation of Highly Stable Organic Glasses

A. Sepúlveda,<sup>1</sup> M. Tylinski,<sup>1</sup> A. Guiseppi-Elie,<sup>2</sup> R. Richert,<sup>3</sup> and M. D. Ediger<sup>1</sup>

<sup>1</sup>*Department of Chemistry, University of Wisconsin-Madison, Madison, Wisconsin 53706, USA*

<sup>2</sup>*Department of Bioengineering, Clemson University, Clemson, South Carolina 29634, USA*

<sup>3</sup>*Department of Chemistry and Biochemistry, Arizona State University, Tempe, Arizona 85287, USA*

(Received 10 January 2014; published 23 July 2014)

*In situ* dielectric spectroscopy has been used to characterize vapor-deposited glasses of methyl-*m*-toluate (MMT), an organic glass former with low fragility ( $m = 60$ ). Deposition near  $0.84T_g$  produces glasses of very high kinetic stability; these materials are comparable in stability to the most stable glasses produced from more fragile glass formers. Highly stable glasses of MMT, when annealed above  $T_g$ , transform into the supercooled liquid by a heterogeneous mechanism. A constant velocity propagating front is initiated at the free surface and controls the transformation of thin films. The transition to a bulk-dominated transformation process occurs at  $5\ \mu\text{m}$ , the largest length scale reported for any glass. Contrary to recent conclusions, we find that physical vapor deposition can form highly stable organic glasses across the entire range of liquid fragilities.

DOI: 10.1103/PhysRevLett.113.045901

PACS numbers: 65.20.Jk, 68.35.bj, 77.55.-g, 81.10.Bk

The recent discovery of highly stable glasses provides an opportunity to explore novel, interesting, and important features of materials. Highly stable glasses can be prepared by means of physical vapor deposition when using an optimal substrate temperature close to  $T_{\text{dep}} \approx 0.85T_g$  ( $T_g$  being the conventional glass transition temperature). Characteristics of these vapor-deposited films, relative to liquid-cooled glasses, include much higher kinetic stability [1,2], lower heat capacity [3,4], lower enthalpy [5,6], higher density [7,8], increased resistance to vapor uptake [9], and anisotropic packing [8,10]. These properties are obtained as a result of the enhanced mobility present at the surface of glasses [11–13] and an intermediate temperature regime where this mobility is large enough to allow near-equilibrium amorphous packing to be attained during the deposition process [14]. Qualitatively, each layer of the glass is efficiently packed and then this packing is locked into place by further deposition [1]. Ordinary glasses would require thousands of years to reach comparable properties either by slowly cooling the liquid or by an aging process [5]. A consequence of the extraordinary stability of these new glassy materials is that, when annealed above  $T_g$ , they transform into the liquid state *heterogeneously* via an unprecedented propagating front of mobility [15,16]. The much faster transformation of ordinary glasses occurs *homogeneously*, characterized by a gradual softening of the entire bulk sample [17]. The features of the homogeneous and heterogeneous transformation regimes have been systematically explored via a facilitated kinetic Ising model [18].

Some systems apparently cannot form stable glasses, and a critical issue for the systematic development of these materials is understanding what material properties are required for stable glass formation. Stable glasses have been prepared from  $\sim 15$  organic molecules, including molecules

with a wide range of size and  $T_g$  values [2,4], poor glass formers [19,20], mixtures [19], and intermediate-to-high fragility systems [16,19,21]. Recent studies have shown that glasses with high kinetic stability can be prepared from other classes of materials, i.e., metals [22,23] and polymers [24]. Computer simulations have reported stable glass properties for both organic and metallic systems [25,26]. In contrast, organic systems with lower fragility and strong hydrogen-bonding networks [27] apparently fail to form stable glasses [28,29].

Recent reports have attempted to establish a correlation between the fragility of a liquid and the ability to form stable glasses [22,29–31]. Fragility, characterized by the steepness index  $m$ , expresses the rate at which the viscosity or relaxation time changes with temperature on cooling towards  $T_g$  [32] and is given by

$$m = \left. \frac{d \log_{10}(\tau_\alpha)}{d(T_g/T)} \right|_{T=T_g}$$

Small and large values of  $m$  are classified as “strong” and “fragile” glass formers, respectively. This concept has been introduced and widely investigated by Angell [33]. Fragility has been found to be associated with some features in glasses such as the heat capacity jump at  $T_g$  [34], the boson peak [35], and features of the potential energy landscape [36].

All molecular systems shown to form stable glasses have intermediate-to-high fragilities and it is not clear at present whether low fragility systems can form highly stable glasses. The most fragile system reported to exhibit stable glass features is a mixture of *cis/trans*-decalin with  $m = 147$  [19]. Thus far, indomethacin (IMC), with an intermediate fragility  $m = 83$ , is the system with the lowest value of fragility reported to form stable glasses [8,16]. Lower fragility organic systems (ethylcyclohexane,

glycerol), both with  $m = 57$ , reportedly fail to form stable glasses [28,29]. Samwer and co-workers [22] compared metallic, polymeric, and molecular stable glasses, with a wide range of fragilities from  $m = 40$  to 145. While glasses with some enhanced kinetic stability were formed across this range, these authors concluded that kinetic stability increased systematically and significantly with fragility. Nakayama *et al.* have independently concluded that high density, a feature often associated with high kinetic stability, is correlated with high fragility [29].

In this Letter, we report that vapor deposition of methyl-*m*-toluate (MMT) forms glasses with very high kinetic stability. To our knowledge, this is the organic glass former with the lowest fragility ( $m = 60$ ) known to form highly stable glasses. We use *in situ* dielectric spectroscopy in conjunction with microlithographically fabricated interdigitated electrode devices to probe the glass characteristics of vapor-deposited thin films of MMT [37–39]. Several other properties associated with high kinetic stability, including a propagating growth front transformation mechanism, were also observed. The transition from a surface-initiated to bulk transformation process occurs at  $5 \mu\text{m}$ , the largest length scale reported for any glass. By comparison with other molecular systems under carefully controlled preparation and transformation conditions, we establish that stable glasses of comparable kinetic stability can be prepared over a wide range of fragilities. This conclusion is consistent with recent predictions of the random first order transition (RFOT) theory [46]. Additional experimental details may be found in the Supplemental Material [38].

Stable glasses of MMT transform to the liquid state heterogeneously when annealed above  $T_g$ . This transformation process is monitored by the increase of the dielectric loss response  $\epsilon''$ . Figure 1 shows the dielectric loss spectra of  $\sim 15 \mu\text{m}$  thick, vapor-deposited, highly stable glasses of MMT as a function of time during isothermal annealing. These samples were deposited at  $T_{\text{dep}} = 142 \text{ K}$  ( $0.84T_g$ ) and subsequently heated to the desired annealing temperature ( $T_{\text{ann}}$ ) within 60 s. The initial spectrum recorded does not show any dielectric loss peak of the primary  $\alpha$ -relaxation process since the well-packed structure of the highly stable glass eliminates mobility in this frequency range; in this sense, highly stable glasses are essentially loss-free materials [39]. The dielectric loss gains amplitude with annealing time consistent with a heterogeneous transformation mechanism; i.e., at any given time, all parts of the sample respond either as the supercooled liquid or as the original stable glass. Consistent with this, fitting  $\epsilon''$  to the empirical Havriliak-Negami [47] function with a fixed value of the characteristic relaxation time  $\tau_\alpha$  provides an excellent description of each data set from the beginning to the end of the transformation process.

The kinetic stability of vapor-deposited MMT glasses strongly depends upon the deposition temperature, consistent with other systems that have shown stable glass

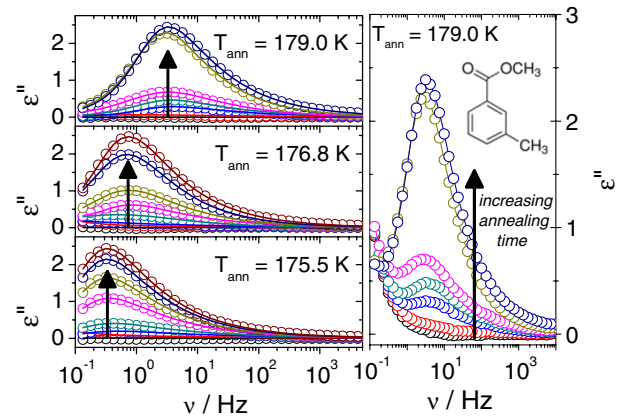


FIG. 1 (color online). Dielectric loss spectra of highly stable methyl-*m*-toluate (MMT) glasses during annealing  $T_{\text{ann}} = 175.5$ , 176.8, and 179.0 K (films  $\sim 15 \mu\text{m}$  thick). The loss amplitude rises from nearly zero with increasing annealing time as the stable glass transforms into the supercooled liquid. The lines are best fits using a fixed relaxation time at each  $T_{\text{ann}}$ . Dielectric spectra (left-hand panels) are obtained by subtracting dc conductivity from the original data (shown in right-hand panel for  $T_{\text{ann}} = 179.0 \text{ K}$ ). Inset: Structure of MMT.

formation. The kinetic stability is best quantified by the glass-to-liquid transformation time ( $t_{\text{trans}}$ ) during isothermal annealing. Figure 2 compares isothermal experiments for  $1.0 \mu\text{m}$  thick films vapor deposited at different

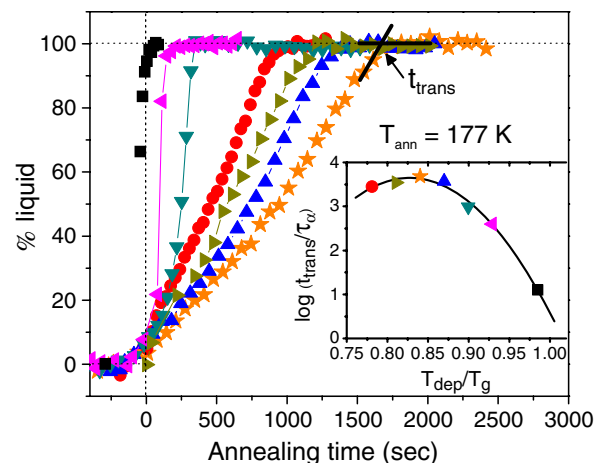


FIG. 2 (color online). Time evolution of the dielectric response of  $1.0 \mu\text{m}$  thick MMT glasses vapor deposited at various temperatures, during annealing at 177 K. The y axis indicates the fraction of sample with the dielectric response of the supercooled liquid, evaluated at 1.77 Hz. Colors and symbols indicate deposition temperatures: 132 K (red circles), 137 K (dark yellow right-side triangles), 142 K (orange stars), 147 K (blue up triangles), 152 K (dark cyan down triangles), 157 K (magenta left-side triangles), and 167 K (black squares). Inset: Time required for complete transformation into the liquid ( $t_{\text{trans}}$ ) as a function of deposition temperature ( $T_{\text{dep}}$ ), divided by the liquid structural relaxation time ( $\tau_\alpha$ ).

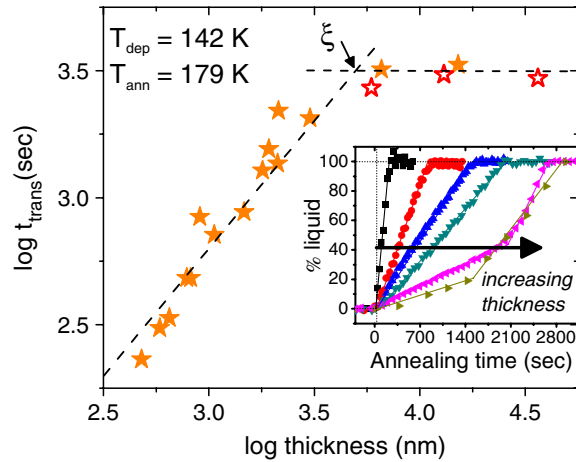


FIG. 3 (color online). Time required to transform stable glasses of MMT ( $t_{\text{trans}}$ ) into the supercooled liquid as a function of film thickness. All films were deposited at 142 K and annealed at 179 K. The transformation time increases linearly with thickness and then becomes constant. Symbols indicate deposition rates: 0.2 nm/s (orange filled stars), 1 nm/s (red open stars). Inset: Subset of the transformation curves that provide  $t_{\text{trans}}$ : 480 nm (black squares), 1.5  $\mu\text{m}$  (red circles), 1.9  $\mu\text{m}$  (blue up triangles), 3  $\mu\text{m}$  (cyan down triangles), 6  $\mu\text{m}$  (magenta left-side triangles), and 35  $\mu\text{m}$  (dark yellow right-side triangles).

$T_{\text{dep}}$ , with the annealing temperature fixed at 177 K. The longest transformation time (maximum stability) for MMT glasses is achieved when using a deposition temperature of  $T_{\text{dep}} = 0.84T_g$ . In the inset of Fig. 2, the transformation time  $t_{\text{trans}}$  is compared to the structural relaxation time of the supercooled liquid  $\tau_\alpha$  at the annealing temperature, since the latter quantity approximately represents the transformation time of an ordinary liquid-cooled glass. By this measure, the most stable vapor-deposited glass of MMT exceeds the stability of an ordinary glass by a factor of  $10^{3.7}$  (for a sample thickness of 1.0  $\mu\text{m}$ ).

The transformation time for highly stable glasses of MMT depends on film thickness, increasing linearly with thickness until a crossover length  $\xi$  of 5  $\mu\text{m}$ . Figure 3 summarizes the transformation times as a function of sample thickness for films between 480 nm and 35  $\mu\text{m}$ , with all films deposited at 142 K and annealed at 179 K. These results clearly show two thickness regimes for highly

stable glasses of MMT. For stable glasses with thickness below  $\xi$ , the molecules are so tightly packed in the interior of the film that no molecular rearrangements happen before a propagating front has transformed the entire sample to the liquid state; this front initiates at the free surface due to enhanced surface mobility. This propagating front moves at a constant velocity as indicated by the approximately linear dependence of transformation time on film thickness (Fig. 3, main panel) and the linear transformation kinetics of individual thin films (Fig. 3, inset). This surface-initiated front mechanism has been directly observed in secondary ion mass spectrometry (SIMS) experiments on stable glasses of IMC and trisnaphthylbenzene (TNB) [16,48], and we interpret our data from this perspective. For stable glasses with thickness above  $\xi$ , the transformation time is independent of film thickness, indicating dominance of a bulk transformation mechanism. The crossover length is an important metric of glass stability; large distances indicate that the local packing has a high activation barrier for rearrangement. The value of  $\xi = 5 \mu\text{m}$  for MMT is the largest reported to date (see Table I).

The velocity of the propagating transformation growth front depends strongly on  $T_{\text{ann}}$ . Growth front velocities ( $V_{\text{gr}}$ ) for this propagating mechanism were calculated by dividing film thickness by  $t_{\text{trans}}$  for samples in the thin film regime. Figure 4 shows the dependence of  $V_{\text{gr}}$  on the annealing temperature, using the structural relaxation time of the supercooled liquid at  $T_{\text{ann}}$  to compare the data for a number of systems. Qualitative similarities can be seen for materials with a wide range of fragilities. For all systems the growth front velocities show a slightly weaker temperature dependence than  $\tau_\alpha$ . This behavior, which collectively covers more than 5 orders of magnitude in  $\tau_\alpha$ , supports the idea that mobility of the liquid adjacent to the stable glass controls the propagating front velocity [46], independent of liquid fragility. In constructing Fig. 4, we used values for  $\tau_\alpha$  obtained from dielectric relaxation measurements on toluene [52], ethylbenzene [31], IMC [49], and TNB [50]. Growth front velocities for IMC and TNB were obtained from SIMS measurements [16] while values for toluene and ethylbenzene were obtained from ac nanocalorimetry [51].

Stable glasses of MMT show features similar to those observed for the most stable glasses formed from systems of higher fragility. Table I summarizes properties of organic

TABLE I. Properties of highly stable organic glasses.  $t_{\text{trans}}$  is the transformation time for a thick film at the temperature where  $\tau_\alpha \approx 1.5$  s for the supercooled liquid.

| Material   | $m$ | $T_g$ (K) | $T_{\text{dep}}$ for maximum stability | $\xi$ ( $\mu\text{m}$ ) | $t_{\text{trans}}/\tau_\alpha$ |
|--|-----|-----------|--|-------------------------|--------------------------------|
| Methyl- <i>m</i> -toluate                            | 60  | 169       | $0.84T_g$                              | $5 \pm 2$               | $10^{4.6}$                     |
| Indomethacin [16,49]                                 | 83  | 315       | $0.84T_g$                              | $1.2 \pm 0.2$           | $10^{4.5}$                     |
| $\alpha, \alpha, \beta$ -trisnaphthylbenzene [16,50] | 86  | 348       | $0.85T_g$                              | $2 \pm 0.5$             | $10^{5.1 \pm 0.3}$             |
| Ethylbenzene [31,51]                                 | 97  | 115       | $0.91T_g$                              | ...                     | $\geq 10^{3.6}$                |
| Toluene [51,52]                                      | 104 | 117       | $0.90T_g$                              | $0.4 \pm 0.1$           | $10^{3.7}$                     |
| 50/50 <i>cis/trans</i> -decalin [19]                 | 145 | 135       | $0.86T_g$                              | ...                     | $\geq 10^{4.4}$                |

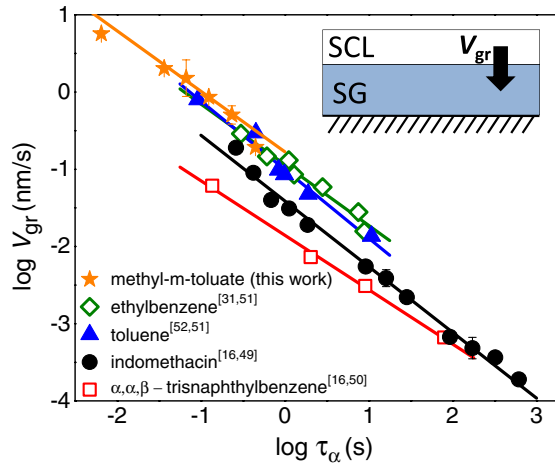


FIG. 4 (color online). Transformation growth front velocities for stable glasses of MMT, ethylbenzene, toluene, IMC, and TNB as a function of the liquid structural relaxation time ( $\tau_\alpha$ ) at the annealing temperature. For MMT, annealing temperatures range from 176 to 183 K. For all systems, the temperature dependence of the growth front velocity is slightly weaker than the temperature dependence of  $\tau_\alpha$ . Inset: Schematic illustration of stable glass (SG) to supercooled liquid (SCL) transformation for thin films.

systems that have been shown to form highly stable glasses. All of these systems have shown maximum kinetic stability for deposition temperatures between  $0.84T_g$  and  $0.91T_g$ . All systems for which this phenomenon has been investigated show a thin film regime where  $t_{\text{trans}}$  increases linearly with film thickness. In particular, the best available metric to evaluate kinetic stability ( $t_{\text{trans}}/\tau_\alpha$ ) shows that, independent of the fragility parameter  $m$ , all these materials are  $\sim 10^4$ – $10^5$  times more stable than ordinary liquid-cooled glasses. Thus, we conclude, for materials carefully prepared and characterized under comparable conditions, there is no evidence that fragility is an important controlling factor for the formation of highly stable glasses.

We place these results within a theoretical context as follows. Highly stable glasses are formed as a result of partial equilibration near the surface during deposition due to enhanced mobility relative to the bulk. If the deposition occurs at the temperature where maximum kinetic stability is reached, the surface relaxation time  $\tau_{\text{surf}}$  should be of the same order of magnitude as the time that the average molecule spends in the surface layer ( $\tilde{d}/k$ , where  $d$  is the molecular diameter and  $k$  is the deposition rate). On the other hand, the most stable glass that can be prepared at a given  $T_{\text{dep}}$  is thought to be the equilibrium supercooled liquid and its kinetic stability is characterized by  $\tau_\alpha$  [14]. From this perspective, the maximum kinetic stability that can be attained for a given molecule is controlled by  $\tau_{\text{surf}}/\tau_\alpha$ , with smaller values associated with greater stability. Stevenson and Wolynes [12] have used the RFOT theory to calculate that  $\tau_{\text{surf}}/\tau_\alpha = \sqrt{\tau_0/\tau_\alpha}$ , where  $\tau_0$  is on

the order of 1 ps. As this prediction is independent of any molecular characteristics, it indicates that glasses of equally high kinetic stability can be attained for liquids across the entire range of possible fragilities. This is in good agreement with the results shown in Table I. The RFOT prediction for surface mobility has been tested against two molecular systems of intermediate fragility, and the results are in reasonable qualitative accord [11]. Further work within the RFOT framework has resulted in predictions for the growth front velocity for TNB stable glasses, and these results are in good agreement with those shown in Fig. 4 [53]. Whether this approach or others can account for the differences between the different systems shown in Fig. 4, or for the very large value of  $\xi$  for MMT, remains to be determined.

In summary, highly stable glasses of methyl-*m*-toluate have been prepared, allowing a systematic comparison of stable glasses associated with liquids covering a wide range of fragility. The transformation mechanism observed when annealing thin films of highly stable glasses of MMT indicates a heterogeneous mechanism governed by a surface-initiated front process. The propagating front velocity for MMT shows a similar temperature dependence when compared to other stable glasses. Thick films also show a heterogeneous transformation into the supercooled liquid. The crossover from thickness-dependent to bulk transformation occurs at  $5 \mu\text{m}$ , the largest length scale reported to date for any glass. The kinetic stability for MMT glasses, quantified as  $t_{\text{trans}}/\tau_\alpha$ , is comparable to values obtained for intermediate-to-high fragility systems.

In contrast to recent reports that fragility defines the ability of a material to form stable glasses, we have shown that comparably stable glasses can be obtained via PVD for a number of organic materials across the entire range of liquid fragilities. Stable glasses allow unprecedented access to the lower portions of the potential energy landscape, and the present finding opens the way to such investigations for strong glass formers. The present results also indicate that liquids across this range of fragility form glasses with high surface mobility. Liquids with strong networks of hydrogen bonds are one group that appears not to form stable glasses. Whether this exception occurs because these liquids do not exhibit enhanced surface mobility or for other reasons remains to be established.

This work was supported by the National Science Foundation under Grant No. CHE-1265737 and by ABTECH Scientific, Inc.

- [1] S. F. Swallen, K. L. Kearns, M. K. Mapes, Y. S. Kim, R. J. McMahon, M. D. Ediger, T. Wu, L. Yu, and S. Satija, *Science* **315**, 353 (2007).
- [2] E. Leon-Gutierrez, A. Sepulveda, G. Garcia, M. T. Clavaguera-Mora, and J. Rodriguez-Viejo, *Phys. Chem. Chem. Phys.* **12**, 14693 (2010).

- [3] K. L. Kearns, M. D. Ediger, H. Huth, and C. Schick, *J. Phys. Chem. Lett.* **1**, 388 (2010).
- [4] M. Ahrenberg, E. Shoifet, K. R. Whitaker, H. Huth, M. D. Ediger, and C. Schick, *Rev. Sci. Instrum.* **83**, 033902 (2012).
- [5] K. L. Kearns, S. F. Swallen, M. D. Ediger, T. Wu, Y. Sun, and L. Yu, *J. Phys. Chem. B* **112**, 4934 (2008).
- [6] S. L. L. M. Ramos, M. Oguni, K. Ishii, and H. Nakayama, *J. Phys. Chem. B* **115**, 14327 (2011).
- [7] S. S. Dalal, A. Sepulveda, G. K. Pribil, Z. Fakhraai, and M. D. Ediger, *J. Chem. Phys.* **136**, 204501 (2012).
- [8] S. S. Dalal and M. D. Ediger, *J. Phys. Chem. Lett.* **3**, 1229 (2012).
- [9] K. J. Dawson, K. L. Kearns, M. D. Ediger, M. J. Sacchetti, and G. D. Zografis, *J. Phys. Chem. B* **113**, 2422 (2009).
- [10] K. J. Dawson, L. Zhu, L. A. Yu, and M. D. Ediger, *J. Phys. Chem. B* **115**, 455 (2011).
- [11] C. W. Brian and L. Yu, *J. Phys. Chem. A* **117**, 13303 (2013).
- [12] J. D. Stevenson and P. G. Wolynes, *J. Chem. Phys.* **129**, 234514 (2008).
- [13] C. R. Daley, Z. Fakhraai, M. D. Ediger, and J. A. Forrest, *Soft Matter* **8**, 2206 (2012).
- [14] S. S. Dalal, Z. Fakhraai, and M. Ediger, *J. Phys. Chem. B* **117**, 15415 (2013).
- [15] S. F. Swallen, K. Traynor, R. J. McMahon, M. D. Ediger, and T. E. Mates, *Phys. Rev. Lett.* **102**, 065503 (2009).
- [16] A. Sepúlveda, S. F. Swallen, L. A. Kopff, R. J. McMahon, and M. D. Ediger, *J. Chem. Phys.* **137**, 204508 (2012).
- [17] S. F. Swallen and M. D. Ediger, *Soft Matter* **7**, 10339 (2011).
- [18] S. Leonard and P. Harrowell, *J. Chem. Phys.* **133**, 244502 (2010).
- [19] K. R. Whitaker, D. J. Scifo, M. D. Ediger, M. Ahrenberg, and C. Schick, *J. Phys. Chem. B* **117**, 12724 (2013).
- [20] K. Dawson, L. A. Kopff, L. Zhu, R. J. McMahon, L. Yu, R. Richert, and M. D. Ediger, *J. Chem. Phys.* **136**, 094505 (2012).
- [21] L. Zhu and L. A. Yu, *Chem. Phys. Lett.* **499**, 62 (2010).
- [22] H. B. Yu, Y. Luo, and K. Samwer, *Adv. Mater.* **25**, 5904 (2013).
- [23] D. P. B. Aji, A. Hirata, F. Zhu, L. Pan, K. M. Reddy, S. Song, Y. Liu, T. Fujita, S. Kohara, and M. Chen, [arXiv:1306.1575](https://arxiv.org/abs/1306.1575).
- [24] Y. L. Guo, A. Morozov, D. Schneider, J. Chung, C. Zhang, M. Waldmann, N. Yao, G. Fytas, C. B. Arnold, and R. D. Priestley, *Nat. Mater.* **11**, 337 (2012).
- [25] I. Lyubimov, M. D. Ediger, and J. J. de Pablo, *J. Chem. Phys.* **139**, 144505 (2013).
- [26] S. Singh and J. J. de Pablo, *J. Chem. Phys.* **134**, 194903 (2011).
- [27] D. Averett, M. T. Cicerone, J. F. Douglas, and J. J. de Pablo, *Soft Matter* **8**, 4936 (2012).
- [28] S. Capponi, S. Napolitano, and M. Wubbenhorst, *Nat. Commun.* **3**, 1233 (2012).
- [29] H. Nakayama, K. Omori, K. Ino-u-e, and K. Ishii, *J. Phys. Chem. B* **117**, 10311 (2013).
- [30] C. A. Angell, in *Structural Glasses and Supercooled Liquids: Theory, Experiment and Applications*, 1st ed., edited by P. G. Wolynes and V. Lubchenko (John Wiley & Sons, New York, 2012), pp. 237–278.
- [31] Z. Chen and R. Richert, *J. Chem. Phys.* **135**, 124515 (2011).
- [32] L. M. Wang, C. A. Angell, and R. Richert, *J. Chem. Phys.* **125**, 074505 (2006).
- [33] C. A. Angell, *Science* **267**, 1924 (1995).
- [34] X. Y. Xia and P. G. Wolynes, *Proc. Natl. Acad. Sci. U.S.A.* **97**, 2990 (2000).
- [35] A. P. Sokolov, E. Rossler, A. Kisliuk and D. Quitmann, *Phys. Rev. Lett.* **71**, 2062 (1993).
- [36] S. Sastry, *Nature (London)* **409**, 164 (2001).
- [37] Z. Chen, A. Sepulveda, M. D. Ediger, and R. Richert, *Eur. Phys. J. B* **85**, 268 (2012).
- [38] See Supplemental Material at <http://link.aps.org/supplemental/10.1103/PhysRevLett.113.045901>, which includes Refs. [28,37,39–45], for detailed description on deposition conditions, dielectric measurement procedure, sample thickness calculation and conductivity corrections.
- [39] Z. Chen, A. Sepúlveda, M. D. Ediger, and R. Richert, *J. Chem. Phys.* **138**, 12A519 (2013).
- [40] L. J. Yang, A. Guiseppi-Wilson, and A. Guiseppi-Elie, *Biomed. Microdevices* **13**, 279 (2011).
- [41] R. Richert, *Rev. Sci. Instrum.* **67**, 3217 (1996).
- [42] Z. M. Chen, Y. Zhao, and L. M. Wang, *J. Chem. Phys.* **130**, 204515 (2009).
- [43] A. I. Nielsen, T. Christensen, B. Jakobsen, K. Niss, N. B. Olsen, R. Richert, and J. C. Dyre, *J. Chem. Phys.* **130**, 154508 (2009).
- [44] M. C. Zaretsky, L. Mouyad, and J. R. Melcher, *IEEE Trans. Electr. Insul.* **23**, 897 (1988).
- [45] L. F. Maia and A. C. M. Rodrigues, *Solid State Ionics* **168**, 87 (2004).
- [46] P. G. Wolynes, *Proc. Natl. Acad. Sci. U.S.A.* **106**, 1353 (2009).
- [47] S. Havriliak and S. Negami, *Polymer* **8**, 161 (1967).
- [48] A. Sepúlveda, S. F. Swallen, and M. D. Ediger, *J. Chem. Phys.* **138**, 12A517 (2013).
- [49] Z. Wojnarowska, K. Adrjanowicz, P. Włodarczyk, E. Kaminska, K. Kaminski, K. Grzybowska, R. Wrzalik, M. Paluch, and K. L. Ngai, *J. Phys. Chem. B* **113**, 12536 (2009).
- [50] R. Richert, K. Duvvuri, and L. T. Duong, *J. Chem. Phys.* **118**, 1828 (2003).
- [51] M. Ahrenberg, Y. Z. Chua, K. R. Whitaker, H. Huth, M. D. Ediger, and C. Schick, *J. Chem. Phys.* **138**, 024501 (2013).
- [52] A. Kudlik, C. Tschirwitz, T. Blochowicz, S. Benkhof, and E. Rossler, *J. Non-Cryst. Solids* **235–237**, 406 (1998).
- [53] A. Wisitsorasak and P. G. Wolynes, *Phys. Rev. E* **88**, 022308 (2013).